Radiation Medicine and Protection 2 (2021) 89–94

Contents lists available at ScienceDirect

Radiation Medicine and Protection

journal homepage: www.radmp.org

Original Article

Study on urine biomarkers of radiation-induced injury guided by *Caenorhabditis elegans* as a model organism

Xin Wu *, Tong Zhu, Hang Li, Xin He, Sai-jun Fan **

Tianjin Key Laboratory of Radiation Medicine and Molecular Nuclear Medicine, Institute of Radiation Medicine, Chinese Academy of Medical Sciences and Peking Union Medical College, Tianjin, 300192, China

ARTICLE INFO

Keywords:
Radiation-induced injury
Model organism
Urine
Metabolomics
Biomarkers

ABSTRACT

Objective: Under the guidance of model organism *Caenorhabditis elegans* with fine olfactory system, small molecular metabolites sensitive to high dose radiation were screened as biomarkers of acute radiation-induced injury, and their metabolic pathways were elucidated by enrichment.

Methods: Rats were irradiated with 12 Gy γ-rays to establish an acute radiation injury model, and their urine was fingerprinted using UPLC-Q/TOF-MS. Further, under the guidance of *Caenorhabditis elegans* as olfactory-sensitive model organism, the key differential metabolites in urine were found as biomarkers of radiation-induced injury.

Results: After rats were irradiated, the radiation injury urine showed a difference from control (sham-irradiated) urine, which could be distinguished by *Caenorhabditis elegans*. Based on metabolomics analysis, a total of 21 key differential metabolites with P value < 0.05 and fold change either >2 or <0.5 were identified, which can be used as sensitive and reliable biomarkers of radiation-induced injury. The pathways were further enriched, and it was found that disorders of five metabolic pathways, including citric acid cycle and amino acid metabolism, play an important role in radiation-induced injury.

Conclusions: Due to radiation injury, the metabolites in urine will change significantly. The study on biomarkers guided by model organism *Caenorhabditis elegans* provides a new perspective to explain the details of metabolic disorders, and also provides experimental basis for the development of new biological dosimeters.

1. Introduction

The development of nuclear technology and nuclear application has greatly increased the chance for people suffering from ionizing radiation. Accidental exposure to ionizing radiation can cause some irreversible pathological changes to the body, and even injure tissues and organs beyond a certain dose or dose rate. In addition, nuclear terrorism and nuclear accidents increase the risk of irradiation, which is also a potential threat.[1,2] It is generally regarded that early and accurate diagnosis of radiation-induced injury should benefit from scientific therapies as soon as possible. However, biodosimetry uses stable chromosomal aberrations for radiologic diagnosis, which is time-consuming and laborious, and has many limitations. Therefore, it is not suitable to rapidly classify whether the people were exposed to ionizing radiation, and estimate biological effects of irradiation injury.[3,4]

Promising candidate biomarkers, including metabolites, have shown great potential for diagnosis in the early stage of diseases.[5] Metabolomics can analyze all metabolites in biological samples through high-throughput detection techniques. Nevertheless, biomarkers based on metabolomics are still at the early phases of development, and various issues need to be addressed, among which huge amount of data and difficulty in screening are the most prominent problems.[6,7] *Caenorhabditis elegans* (*C. elegans*) has a fine olfactory system, which is characterized by the nervous system composed of only 302 neurons. *C. elegans* displays chemo-attractive responses, not only can sense hundreds of molecules, but also have different behaviors to different concentrations of the same molecules. As a model organism, *C. elegans* is sensitive to the urine of radiation injured rats, which is worthy of attention.[8–10] We try to apply this model organism for guidance to rapidly and simply screen key differentially expressed metabolites as biomarkers.

In this study, we first used olfactory-sensitive *C. elegans* to diagnose whether the urine from radiation injured rats, so as to speculate that

* Corresponding author. Institute of Radiation Medicine, Chinese Academy of Medical Sciences and Peking Union Medical College, Tianjin Key Laboratory of Radiation Medicine and Molecular Nuclear Medicine, Tianjin, 300192, China.
** Corresponding author.
E-mail addresses: wuxin@irm-cams.ac.cn (X. Wu), fansaijun@irm-cams.ac.cn (S.-j. Fan).

https://doi.org/10.1016/j.radmp.2021.08.001
Received 7 July 2021; Received in revised form 9 August 2021; Accepted 10 August 2021
Available online 11 August 2021

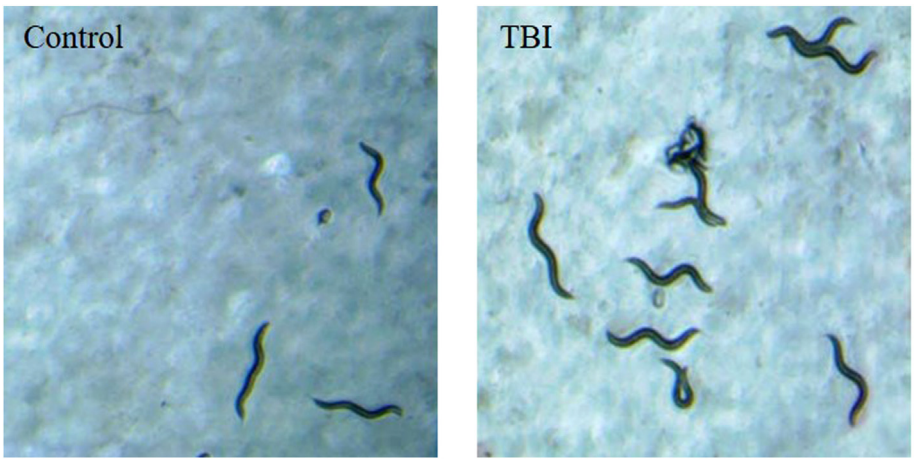

Fig. 1. *C. elegans* tropism to TBI rat urine. *C. elegans* response was visualized under the microscope. *C. elegans* showed significant attraction to urine of TBI rats compared with control rats.

there might be some metabolites attracting *C. elegans* in radiation injury urine. Then, urine samples were fingerprinted using ultra-performance liquid chromatography-quadrupole time-of-flight mass spectrometry (UPLC-Q/TOF-MS) to screen differentially expressed metabolites based on metabolomics. Furthermore, under the guidance of *C. elegans*, the key differential metabolites were found as urine biomarkers of radiation-induced injury. These biomarkers can help to classify the population exposed to ionizing radiation and evaluate biological effects of irradiation injury. This work also provides a new and convenient method to identify biomarkers, which is of great significance for discovering biomarkers of disease and toxicity clinically.

2. Materials and methods

2.1. Animals and treatment

Male Wistar rats, weighing (200 ± 20) g, were supplied by the Institute of Radiation Medicine, Chinese Academy of Medical Sciences (Tianjin, China). Animals were housed in standard cages with free access to water and standard diet, and acclimatized to the facilities for one week. The room was controlled with temperature at (25 ± 2)°C, relative humidity of (50 ± 5) %, and 12/12 h dark-light cycle. Prior to the experiment, all animals were fasted for 12 h, but with free access to water. This study was approved by the steering committee and conducted under the guidelines for clinical studies of Institute of Radiation Medicine, Chinese Academy of Medical Sciences and Peking Union Medical College.

The rats were randomly divided into two groups, eight rats in each group. The radiation group was treated with 12 Gy ^{137}Cs γ-rays for total body irradiation (TBI), and the control group was given 0 Gy sham-irradiation. All rats were returned to special cages with urine and faeces separation device for collecting urine.

2.2. C. elegans maintenance and synchronization

C. elegans strains were cultured on nematode growth medium (NGM) plates at 20°C under standard conditions, coated with a thick layer of *E. coli* OP50 as food.[11] After incubation, the eggs were collected during oviposition period, and then cultured to young adults under conventional conditions to synchronize the growth period. The adult *C. elegans* in synchronous growth period were used for further chemotaxis assays.

2.3. Chemotaxis assays

The chemotaxis assays were conducted on NGM plates. A square of equal length and width was drawn at the corner equidistant from the center of the circle, and 10 μL urine from control and TBI rats were dripped respectively. Approximately 200 synchronized young adults were added at the center of the circle. Then, the number of *C. elegans* in the square on both sides was recorded under microscope.

2.4. Sample preparation

Urine samples were collected for 48 h after irradiation. Sodium azide was added into the collection tube to inhibit the growth of bacteria. The supernatant was centrifuged at 3,000 r/min for 5 min and stored at −20°C until analysis.

C. elegans in the squares corresponding to two groups of urine were collected from chemotaxis assays and placed in a centrifuge tube respectively, and cleaned with precooled buffer solution for 2–3 times to remove bacteria and urine on the surface. After centrifugation at a low speed of 1,200 r/min for 3 min, the precipitates were frozen in liquid nitrogen and crushed on ice by ultrasonic wave, and then treated properly for injection analysis.

2.5. LC-MS conditions

Chromatographic separation was performed on a Waters Acquity UPLC system equipped with a BEH C18 column (2.1 × 100 mm, 1.7 μm). The mobile phase consisted of 0.1% formic acid-water (A) and 0.1% formic acid-acetonitrile (B) at the flow rate of 0.45 mL/min. The gradient program was as follows: 0–0.5 min, 1% B; 0.5–10 min, 1–40% B; 10–11 min, 40%–99% B; and 11–12 min, 99% B. The column temperature was controlled at 40°C, and the injection volume was set to 10 μL.

Mass spectrometric detection was conducted on a Waters Xevo G2-XS QTOF system equipped with an electrospray ionization (ESI) interface. The capillary voltage was 3.0 kV in positive ion mode and 2.0 kV in negative ion mode. High purity nitrogen was used to assist spray ionization and desolvation. Other instrument parameters were as follows: sample cone voltage of 40 V; source temperature of 120°C; desolvation temperature of 450°C; cone gas flow of 50 L/h and desolvation gas flow of 800 L/h. Full-scan analysis was performed in the mass range of m/z 50-1,000.

2.6. Data acquisition and processing

After UPLC-Q/TOF-MS detection, the raw data files were processed by Waters Markerlynx software for ion extraction, peak alignment, normalization and isotope elimination. The converted data corresponding to control and TBI group were imported into SIMCA-P 13.0 for

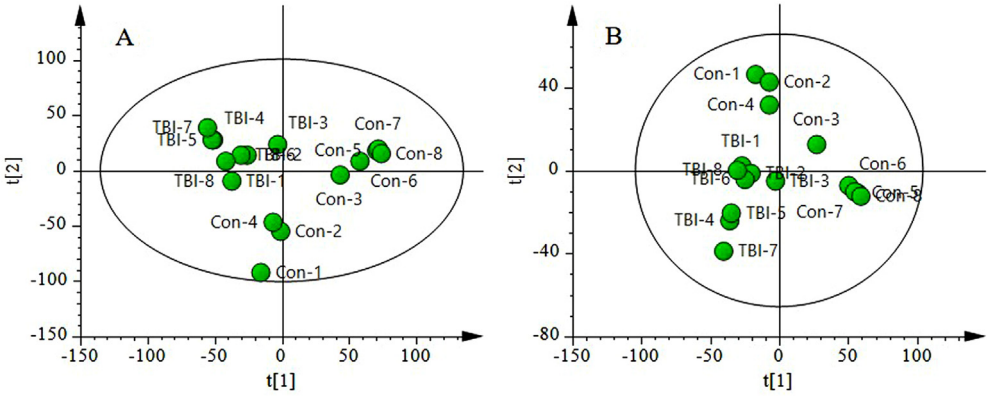

Fig. 2. PCA statistical analysis on urine metabolic profiles. PCA score plots showed that urine samples from TBI rats and control rats were separated in positive (A) and negative (B) ion modes.

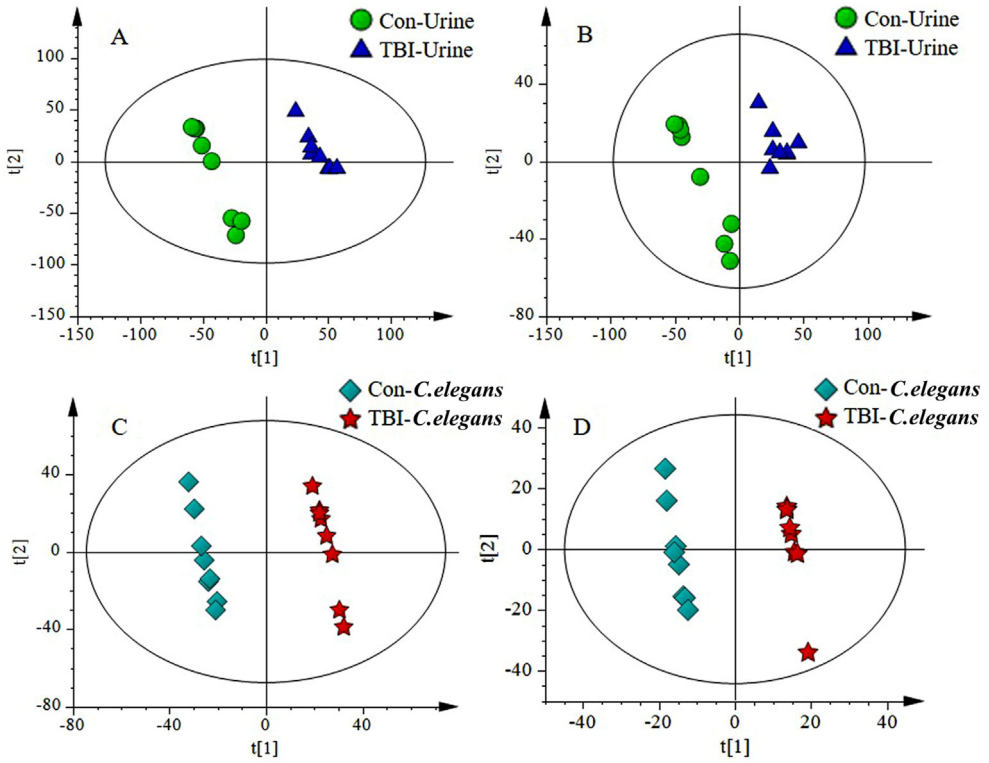

Fig. 3. PLS-DA analysis on urine and *C. elegans* fingerprints. PLS-DA score plots of urine samples from TBI rats (blue triangle) and control rats (green dot) in positive (A) and negative (B) ion modes. PLS-DA score plots of *C. elegans* samples corresponding to TBI urine (red star) and control urine (cyan square) in positive (c) and negative(D) ion modes.

multivariate statistical analysis of principal component analysis (PCA) and partial least squares discriminant analysis (PLS-DA). Then, the differential metabolite ions with variable importance in projection (VIP) value > 1 were submitted to the Venn diagram to screen the common ion signals in urine and *C. elegans* samples. With SPSS software for Student's t-test, the ions with significant difference (P value < 0.05 and fold change either >2 or <0.5) were found, which were produced by biomarkers of radiation-induced injury.

2.7. Biomarker identification and pathway enrichment

The accurate mass of biomarker ions was searched in HMDB (http://www.hmdb.ca/) and Chemspider (http://www.chemspider.com) databases to match the possible compounds. Furthermore, their chemical structures were identified according to the fragment ions in MS spectra. Through KEGG (http://www.genome.jp/kegg/) database, we performed a metabolic pathway enrichment analysis of all identified biomarkers.

3. Results

3.1. C. elegans can distinguish irradiation injury urine

Due to the lack of auditory and visual systems, *C. elegans* have evolved a highly developed olfactory system to sense food and environmental information. Therefore, it is especially suitable for the discrimination of chemical signal differences. As shown in Fig. 1, the number of *C. elegans* in the urine area of TBI group was significantly higher than that of control group, indicating that *C. elegans* could distinguish irradiation injury urine. It can be inferred that there were significant differences in urine

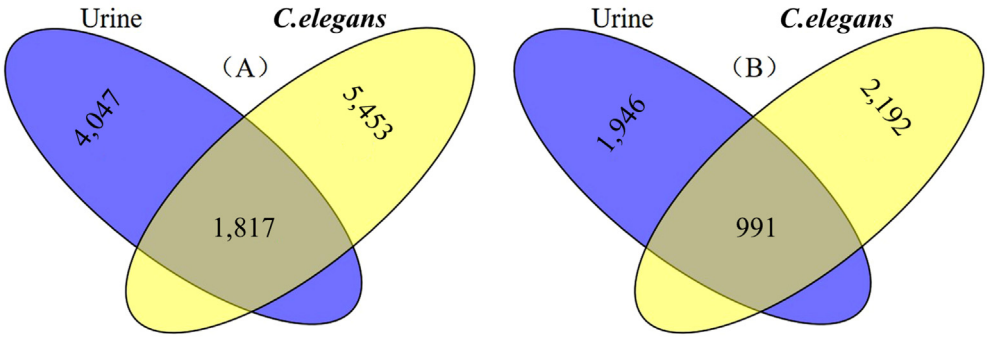

Fig. 4. Venn diagram of differential metabolite ions in urine and *C. elegans*. By visual integration, the differential metabolite ions common to urine and *C. elegans* samples were obtained in positive (A) and negative (B) ion modes.

Table 1
Differentially expressed biomarkers in irradiation injury urine.

No.	t_R (min)	Obsd Ion	Detected	Expected	Error (ppm)	Formula	MS Fragmentation	Metabolite	Content change (TBI/Con)
1	0.43	$[M+K]^+$	160.9649	160.9669	−12.42	$C_3H_6O_3S$	123,105,87	3-Mercaptolactic acid	↑
2	0.63	$[M+H]^+$	132.0773	132.0768	3.79	$C_4H_9N_3O_2$	115,114,90	Beta-Guanidinopropionic acid	↑
3	0.64	$[M+H]^+$	190.1180	190.1186	−3.16	$C_7H_{15}N_3O_3$	130,84,61	Homocitrulline	↓
4	0.66	$[M-H]^-$	191.0194	191.0197	−1.57	$C_6H_8O_7$	173,147,87	Citric acid	↓
5	0.68	$[M+H]^+$	288.1192	288.1190	0.69	$C_{11}H_{17}N_3O_6$	270,139,110	*N*-Ribosylhistidine	↑
6	0.92	$[M+H–H_2O]^+$	143.1187	143.1185	1.40	$C_7H_{16}N_2O_2$	161,115,87	Isoputreanine	↑
7	1.24	$[M+Na]^+$	215.0167	215.0162	2.33	$C_6H_8O_7$	193,145,129	D-Glucaro-1,4-lactone	↓
8	1.24	$[M-H]^-$	191.0190	191.0197	−3.66	$C_6H_8O_8$	173,129,117	Isocitric acid	↓
9	3.47	$[M+H–H_2O]^+$	155.0818	155.0821	−1.93	$C_7H_{12}N_2O_3$	142,116,98	Glycylproline	↓
10	3.64	$[M-H]^-$	315.0717	315.0722	−1.59	$C_{13}H_{16}O_9$	297,170,109	3,4,5-trihydroxy-6-(2-hydroxy-6-methoxyphenoxy)oxane-2-carboxylic acid	↓
11	3.98	$[M+H]^+$	261.1440	261.1445	−1.91	$C_{11}H_{20}N_2O_5$	215,169,86	gamma-Glutamylleucine/gamma-Glutamylisoleucine	↓
12	4.29	$[M-H]^-$	204.0296	204.0302	−2.94	$C_{10}H_7NO_4$	160,158,93	Xanthurenic acid	↑
13	5.23	$[M+HCOO]^-$	299.0765	299.0762	1.00	$C_6H_{15}N_4O_5P$	253,235,173	L-Phosphoarginine	↓
14	5.58	$[M+H]^+$	377.1457	377.1442	3.98	$C_{16}H_{24}O_{10}$	359,215,197	(1x,2x)-Guaiacylglycerol 3-glucoside	↓
15	6.03	$[M+H]^+$	99.0810	99.0810	0.00	$C_6H_{10}O$	99,83,69	3-Hexenal	↑
16	6.10	$[M+H]^+$	181.0859	181.0859	0.00	$C_{10}H_{12}O_3$	165,135,91	3-Methoxybenzenepropanoic acid	↑
17	6.64	$[M-H]^-$	224.0924	224.0928	−1.78	$C_{11}H_{15}NO_4$	164,88,70	(2 S)-2-amino-3-(4-hydroxy-3-methoxyphenyl)-2-methylpropanoic acid	↓
18	7.53	$[M-H]^-$	203.1279	203.1289	−4.92	$C_{10}H_{20}O_4$	185,173,143	3,7-Dimethyl-3-octene-1,2,6,7-tetrol	↑
19	8.26	$[M-H]^-$	253.0498	253.0500	−0.79	$C_7H_{14}N_2O_6S$	209,124,80	5-L-Glutamyl-taurine	↓
20	8.60	$[M-H]^-$	283.0604	283.0606	−0.71	$C_{16}H_{12}O_5$	267,255	Melanettin	↓
21	9.54	$[M-H]^-$	269.0449	269.0455	−2.23	$C_{15}H_{10}O_5$	227,151,117	5,7-dihydroxy-2-(3-hydroxyphenyl)-4H-chromen-4-one	↓

between the two groups.

3.2. LC-MS fingerprint and metabolomics analysis

Urine and *C. elegans* samples were detected by UPLC-Q/TOF-MS to analyze the chemical fingerprints of small molecular metabolites. After fingerprint data conversion, urine samples were first subjected to unsupervised PCA analysis to determine the difference between TBI and control group. According to PCA score plot (Fig. 2), the urine of two groups were distributed in different areas in both positive and negative ion modes, indicating that the metabolites in rat urine were significantly changed due to irradiation injury.

With supervised PLS-DA analysis, metabolomics can reduce the dimension of huge fingerprint data to determine the differential metabolites in radiation injury urine. As shown in Fig. 3A and B, multivariate statistical model fitted well, which ensured the accuracy of metabolomics analysis. Similarly, *C. elegans* samples from chemotaxis assays were imported into PLS-DA analysis. The results showed that chemical fingerprint data were significantly different (Fig. 3C and D), indicating that model organism *C. elegans* was helpful to screen the key biomarkers in radiation injury urine.

For PLS-DA analysis, VIP value was a coefficient reflecting the importance of variables to model discrimination. The metabolite ions with VIP >1 in urine and *C. elegans* samples were screened respectively, and then introduced into Venn diagram for visualization to obtain differential ions in common. As a result (Fig. 4), in positive mode, there were 4,074 differential ions in urine and 5,453 in *C. elegans* samples, including 1817 common ions; and in negative mode, there were 1,946 differential ions in urine and 2,192 in *C. elegans* samples, including 991 common ions. Further, according to P value < 0.05 and fold change of abundance either >2 or <0.5, 24 ions in positive mode and 18 ions in negative mode were found with significant differences, which were considered as urine biomarkers of irradiation injury.

3.3. Identification of urine biomarkers

As mentioned in above analysis, a total of 42 biomarkers ions of radiation-induced injury were found in positive and negative modes. We searched HMDB and Chemspider databases with accurate mass to match the possible endogenous metabolites, and then identified their chemical structures according to the fragment ions in mass spectra. As shown in Table 1, there are 11 compounds in positive ion mode and 10 compounds in negative ion mode, totally 21 differential metabolites as biomarkers of irradiation injury.

Table 2
The details of biomarkers pathways enrichment.

Pathway Name	Total	Expected	Hits	-log$_{10}$(p)	FDR	Impact
Citrate cycle (TCA cycle)	20	0.1193	2	2.2453	0.4775	0.1035
Glyoxylate and dicarboxylate metabolism	32	0.1909	2	1.8447	0.6005	0.0385
Taurine and hypotaurine metabolism	8	0.0477	1	1.3294	1	0
Alanine, aspartate and glutamate metabolism	28	0.1670	1	0.8083	1	0.0323
Cysteine and methionine metabolism	33	0.1968	1	0.7426	1	0

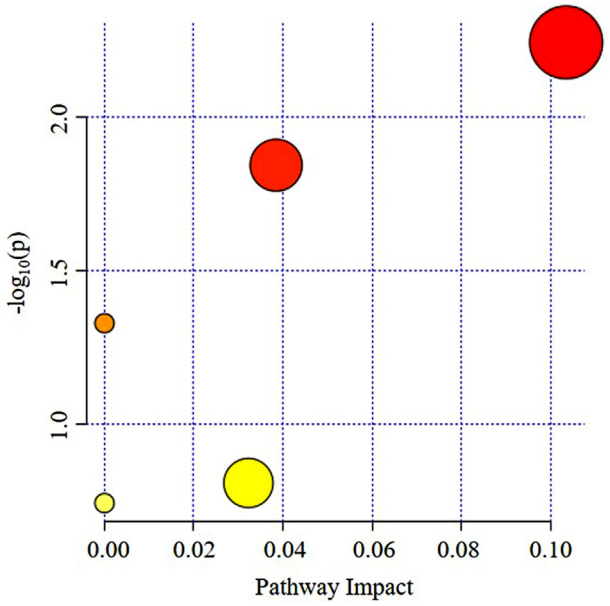

Fig. 5. Summary of metabolic pathway analysis. The horizontal axis was pathway impact value, representing the importance of metabolic pathways, and Vertical axis was logarithm of *P* value calculated by enrichment analysis.

3.4. Metabolic pathway enrichment analysis

With the identified biomarkers, we enriched metabolic pathways (Table 2) and explored the details of metabolic disorders caused by irradiation injury. In the bubble chart (Fig. 5), the abscissa was pathway impact value, representing the importance of metabolic pathway, and the ordinate was logarithm of *P* value in enrichment analysis. The closer metabolic pathway is to the top right in bubble chart, that is, the larger abscissa and ordinate values are, indicating that the higher credibility of the pathway, and the more affected by metabolites.

4. Discussion

Exposure to high-dose ionizing radiation can directly or indirectly cause tissue and organ injuries, and induce a series of oxidative stress reactions, leading to dysfunction and metabolic disorders.[12,13] Once a large-scale irradiation event occurs, it is critical to quickly distinguish the "risk" population and carry out reasonable clinical guidance and treatment. Unfortunately, due to individual differences or delayed responses, symptoms cannot be immediately applied to the diagnosis of most affected population.[14,15] Biomarkers based on metabolomics can quickly detect metabolites and classify the irradiated population before symptoms appear. However, metabolomics data are huge and complex, which cause a lot of inconvenience and labor-intensive in the screening and identification of differential metabolites.[16,17] Under the guidance of model organism *C. elegans*, we can quickly and accurately find the key biomarkers of irradiation injury and explain the details of metabolic pathway disorders using multivariate statistical analysis.

It was found that there were differences between the urine fingerprints of radiation injury and control rats, which total body irradiation rats were used as the model of acute radiation injury. *C. elegans* could significantly distinguish the differences. Twenty-one differential metabolites were screened and identified as urine biomarkers of radiation-induced injury based on *C. elegans* guiding metabolomics. Biodosimetry is the preferred method to assess the exposure dose when nuclear event occurs, while the dicentric assay is currently impractical for large-scale diagnosis because it is too time-consuming and traumatic.[18] In contrast, the key urinary biomarkers guided by *C. elegans* can reflect irradiation injury more intuitively and accurately. This convenient and rapid method is more conducive to large-scale classification and treatment of patients.

Through the enrichment analysis of biomarkers, five metabolic disorder pathways were involved, including citric acid cycle; glyoxylate and dicarboxylate metabolism; taurine and hypotaurine metabolism; alanine, aspartate and glutamate metabolism; cysteine and methionine metabolism. Citric acid and isocitric acid are important intermediates of the tricarboxylic acid cycle, which is the most important energy metabolic process in the body, and is the common metabolic pathway of carbohydrate, fat and protein. In addition, tricarboxylic acid cycle provides precursors for many biosynthetic pathways and is the central link of metabolism.[19,20] In this study, metabolic biomarkers and disordered pathways suggest that irradiation injury may interfere with energy metabolism through the tricarboxylic acid cycle. The biomarkers we identified are also involved in the metabolism of glyoxylic acid and dicarboxylic acid, alanine, aspartic acid and glutamic acid. Radiation exposure causes mitochondrial reprogramming and changes in energy metabolism. The abnormal metabolism of glutamine produces α-ketoglutarate, which enters the tricarboxylic acid cycle and induces metabolic disorder, thus affecting energy metabolism.[21] Therefore, irradiation injury is closely related to the disorder energy metabolism in multiple targets and pathways.

In conclusion, based on metabolomics analysis guided by model organism *C. elegans*, it can quickly, accurately and high-throughput screen out the key biomarkers of radiation injury in urine. Urine has the characteristics of non-invasive collection, which is easier to obtain than plasma, and has advantages over traditional biological dosimeters. This study provides a new perspective to explain the metabolic disorder details of radiation injury, and also provides an experimental basis for the development of new biological dosimeters.

Conflict of interest

The authors have no conflicts of interest to declare.

Acknowledgement

This work was supported by the grants from the National Natural Science Foundation of China (Nos. 81572969 and 81730086).

References

1. Cui M, Xiao H, Li Y, et al. Faecal microbiota transplantation protects against radiation-induced toxicity. *EMBO Mol Med.* 2017;9(4):448–461. https://doi.org/10.15252/emmm.201606932.
2. Xiao C, He N, Liu Y, et al. Research progress on biodosimeters of ionizing radiation damage. *Radiat Med Prot.* 2020;1(3):127–132. https://doi.org/10.1016/j.radmp.2020.06.002.
3. Song M, Xie D, Gao S, et al. A biomarker panel of radiation-upregulated miRNA as signature for ionizing radiation exposure. *Life.* 2020;10(12):361. https://doi.org/10.3390/life10120361.

4. Gramatyka M, Sokół M. Radiation metabolomics in the quest of cardiotoxicity biomarkers: the review. *Int J Radiat Biol*. 2020;96(3):349–359. https://doi.org/10.1080/09553002.2020.1704299.
5. Loke SY, Lee ASG. The future of blood-based biomarkers for the early detection of breast cancer. *Eur J Canc*. 2018;92:54–68. https://doi.org/10.1016/j.ejca.2017.12.025.
6. Zhao M, Lau KK, Zhou X, et al. Urinary metabolic signatures and early triage of acute radiation exposure in rat model. *Mol Biosyst*. 2017;13(4):756–766. https://doi.org/10.1039/c6mb00785f.
7. van der Laan T, Dubbelman AC, Duisters K, et al. High-throughput fractionation coupled to mass spectrometry for improved quantitation in metabolomics. *Anal Chem*. 2020;92(21):14330–14338. https://doi.org/10.1021/acs.analchem.0c01375.
8. Yu Y, Zhi L, Guan X, et al. FLP-4 neuropeptide and its receptor in a neuronal circuit regulate preference choice through functions of ASH-2 trithorax complex in Caenorhabditis elegans. *Sci Rep*. 2016;6:21485. https://doi.org/10.1038/srep21485.
9. Min H, Sung M, Son M, et al. Transgenerational effects of proton beam irradiation on Caenorhabditis elegans germline apoptosis. *Biochem Biophys Res Commun*. 2017;490(3):608–615. https://doi.org/10.1016/j.bbrc.2017.06.085.
10. Kuzmic M, Galas S, Lecomte-Pradines C, et al. Interplay between ionizing radiation effects and aging in C. elegans. *Free Radic Biol Med*. 2019;134:657–665. https://doi.org/10.1016/j.freeradbiomed.2019.02.002.
11. Choi MK, Liu H, Wu T, et al. NMDAR-mediated modulation of gap junction circuit regulates olfactory learning in *C. elegans*. *Nat Commun*. 2020;11(1):3467. https://doi.org/10.1038/s41467-020-17218-0.
12. Zhang J, Han X, Zhao Y, et al. Mouse serum protects against total body irradiation-induced hematopoietic system injury by improving the systemic environment after radiation. *Free Radic Biol Med*. 2019;131:382–392. https://doi.org/10.1016/j.freeradbiomed.2018.12.021.
13. Dong S, Lyu X, Yuan S, et al. Oxidative stress: a critical hint in ionizing radiation induced pyroptosis. *Radiat Med Prot*. 2020;1(4):179–185. https://doi.org/10.1016/j.radmp.2020.10.001.
14. Obrador E, Salvador R, Villaescusa JI, et al. Radioprotection and radiomitigation: from the bench to clinical practice. *Biomedicines*. 2020;8(11):461. https://doi.org/10.3390/biomedicines8110461.
15. Mu H, Sun J, Li L, et al. Ionizing radiation exposure: hazards, prevention, and biomarker screening. *Environ Sci Pollut Res Int*. 2018;25(16):15294–15306. https://doi.org/10.1007/s11356-018-2097-9.
16. Zhang Y, Zhou X, Li C, et al. Assessment of early triage for acute radiation injury in rat model based on urinary amino acid target analysis. *Mol Biosyst*. 2014;10(6):1441–1449. https://doi.org/10.1039/c3mb70526a.
17. Lee HJ, Kremer DM, Sajjakulnukit P, et al. A large-scale analysis of targeted metabolomics data from heterogeneous biological samples provides insights into metabolite dynamics. *Metabolomics*. 2019;15(7):103. https://doi.org/10.1007/s11306-019-1564-8.
18. Flegal FN, Devantier Y, McNamee JP, et al. Quickscan dicentric chromosome analysis for radiation biodosimetry. *Health Phys*. 2010;98(2):276–281. https://doi.org/10.1097/HP.0b013e3181aba9c7.
19. Khan AR, Rana P, Devi MM, et al. Nuclear magnetic resonance spectroscopy-based metabonomic investigation of biochemical effects in serum of γ-irradiated mice. *Int J Radiat Biol*. 2011;87(1):91–97. https://doi.org/10.3109/09553002.2010.518211.
20. Konieczna A, Szczepańska A, Sawiuk K, et al. Effects of partial silencing of genes coding for enzymes involved in glycolysis and tricarboxylic acid cycle on the enterance of human fibroblasts to the S phase. *BMC Cell Biol*. 2015;16:16. https://doi.org/10.1186/s12860-015-0062-8.
21. Kim EJ, Lee M, Kim DY, et al. Mechanisms of energy metabolism in skeletal muscle mitochondria following radiation exposure. *Cells*. 2019;8(9):950. https://doi.org/10.3390/cells8090950.